Ab initio determination of structure-property relationships in alloy nanoparticles

Tim Mueller

Phys. Rev. B **86**, 144201 — Published 11 October 2012

DOI: 10.1103/PhysRevB.86.144201

Ab-initio determination of structure-property relationships in alloy nanoparticles

Tim Mueller*

Johns Hopkins University

101E Maryland Hall
3400 N. Charles Street
Baltimore, MD 21218
tmueller@jhu.edu
(617) 642-6476

Abstract

I present a highly accurate computational study on atomic order in 2-nm cuboctahedral Au-Pd nanoparticles. Equilibrium atomic structures, energies and electronic surface *d*-band centers have been calculated across the entire range of compositions at different temperatures using a Bayesian approach to cluster expansions. The estimated prediction error in formation energies calculated by the cluster expansion, relative to density functional theory, is approximately 1 meV / atom. This prediction error would be low for a cluster expansion on a bulk material, and it is exceptionally low for a study of nanoparticles of this size. This result was accomplished by extending the Bayesian approach for cluster expansions to account for non-local, composition-dependent effects that might otherwise not be captured. For this system the Bayesian approach is estimated to be approximately five times as efficient as more common cluster selection techniques.

PACS Codes

61.50.Ah, 61.66.Dk, 61.46.-w

Atomic order in nanoscale materials plays an important role in a variety of emerging technologies, including lithium-ion batteries,[1] data storage,[2] and catalysis.[3, 4] One of the great challenges in the design of new nanoscale materials is the determination of how atomic order affects their properties.[5] Experimental characterization of the atomic structure of nanoscale materials can be very difficult, and computational methods developed to study bulk crystals can become prohibitively expensive when applied to nanoscale materials due to the loss of translational symmetry. In this communication, I demonstrate how this computational expense can be dramatically reduced by using machine learning techniques to address the particular challenges posed by nanoscale materials. As a result, it becomes feasible to very rapidly and accurately evaluate the properties of nanoscale materials as a function of atomic order. I demonstrate this method by predicting the structures, energies, and centers of the electronic surface *d*-band for 2-nm cuboctahedral Au-Pd nanoparticles across the entire composition range with an estimated accuracy of 1 meV / atom relative to density functional theory (DFT).[6]

My approach is an extension of the cluster expansion method that has been widely used to study atomic order in bulk compounds.[7] The cluster expansion method is applicable to materials such as fcc alloys in which the general topology of atomic sites is known but the ordering of atoms on those sites is not. I will use a binary alloy nanoparticle as an illustration, and it is straightforward to extend the approach to the general case. To start, each atomic site in the crystal is assigned a site variable, s_i. These site variables are similar to spin variables in an Ising model,[8] but in an A-B alloy the value $s_i = 1$ indicates element A is present at the i^{th} site, and $s_i = -1$ indicates element B is present. A

property of the material may then be expressed as a function of these site variables, $F(\mathbf{s})$. The function $F(\mathbf{s})$ is expanded as a linear combination of basis functions, each of which is the product of a cluster of site variables:

$$F(\mathbf{s}) = V_0 + \sum_{clusters} V_{cluster} \prod_{i \in cluster} s_i \qquad (1)$$

where the $V_{cluster}$ are unknown coefficients known as effective cluster interactions (ECI), and V_0 is a constant term representing the "empty" cluster. An example of a cluster of sites might be a nearest-neighbor pair of sites, and the number of sites in a cluster may range from zero to all the sites in the material. When all possible clusters are included, the expansion in equation (1) is exact.

Because it is usually impractical to determine values for all ECI in a cluster expansion, it is common to reduce the expansion so that values only need to be determined for a manageable number of distinct ECI. One way to reduce the number of distinct ECI is to take advantage of the symmetry of the material. For example, in a bulk FCC alloy all nearest-neighbor pairs are symmetrically equivalent, so they all must have the same ECI values. It is also possible to "truncate" the cluster expansion, by recognizing that the ECI for clusters with a large number of sites, or a large distance between sites, are typically very small. It is commonly assumed that these ECI may be set to zero, effectively removing the clusters from the expansion, with little loss of accuracy. The selection of which clusters to include in the expansion is usually accomplished by minimizing the cross-validation error in a set of training data,[9] and a least-squares fit is used to assign values to the ECI. The resulting expansion makes it computationally feasible to very

rapidly predict property values for a large number of atomic configurations, enabling thermodynamic averaging over configurations and combinatorial searches for structures with optimal property values.

The cluster expansion approach has previously been used to model atomic order in bulk materials and predict the shape of nanoparticles,[10, 11] but modeling internal atomic order in nanoparticles is substantially more challenging. Because the symmetry of a nanoparticle is much lower than that of a bulk material, there are many more symmetrically distinct, significant ECI in a nanoparticle. When using a least squares fit, it is necessary to include at least as many structures in the training set as there are unknown ECI, resulting in the need for large training sets. In addition, the low symmetry of the nanoparticle makes the calculation of the property value much more expensive for each element in the training set. The combination of these effects can make it prohibitively expensive to generate sufficient training data. This problem can be alleviated through the use of a Bayesian cluster expansion, in which a prior probability distribution is assigned to ECI values and cross-validation is used to optimize the shape of the distribution.[12] Among the benefits of this approach is that it allows for an arbitrarily large number of ECI to be included in the expansion, regardless of the training set size. The prior probability distribution can be used to couple the ECI between clusters of sites that are congruent but not symmetrically equivalent. For example, it may be supposed *a priori* that the ECI for a nearest-neighbor pair three layers below the nanoparticle surface should be close the ECI for a nearest-neighbor pair four layers below the surface.

It has previously been demonstrated that the Bayesian approach significantly reduces the size of the training set required to fit a cluster expansion to both bulk and nanoparticle energies calculated by the embedded-atom method.[12, 13] However real alloys are more challenging, as they include non-local electronic effects. The need to better represent non-local effects in cluster expansions has been discussed elsewhere,[14] and a proposed solution is to use a composition-dependent linear transformation of the basis functions to reduce the number of significant ECI in the cluster expansions.[15-17] This approach is effective because, as in the Bayesian approach, the resulting cluster expansion can include interactions from more distinct clusters of sites than there are structures in the training set. However, in practice both approaches rely on the evaluation of interactions for a finite number of clusters up to a maximum cluster size, making it difficult to capture truly non-local contributions to the energy.

Some contributions to the energy are composition-dependent, and these are poorly represented by a sum of local interactions. For example, in the Au-Pd nanoparticles considered in this communication, when the number of gold atoms (out of 201 total atoms) reaches 190, an electronic energy level is completely filled, and the next available electronic energy level is calculated to be 275±27 meV higher in energy. This gap was observed in over 20 different nanoparticles with the same composition, regardless of atomic order. The 191st gold atom contributes an extra valence electron that enters this high-energy level, resulting in a discrete jump in the particle energy as a function of composition.

Such composition-dependent contributions to the energy can be addressed by modifying the cluster expansion method, resulting in expansions that are able to rapidly predict the formation energies of Au-Pd nanoparticles across the entire range of compositions with accuracy of about 1 meV/atom. I accomplish this by replacing the constant term V_0 with composition-dependent terms $V_{0,n}$, where n is the number of gold atoms in the nanoparticle. For a 201-atom gold nanoparticle, this approach introduces an additional 201 unknown variables to the cluster expansion. If these terms were independent of one another, very large training sets would be required to determine the values of $V_{0,n}$ at each possible composition. However it may be expected that the ECI values for compositions that are close to each other must also be close. To enforce this expectation, I use the Bayesian prior distribution to couple empty ECI values, much in the same way the Bayesian prior distribution is used to couple the values of the ECI for congruent clusters. Specifically, for the 201-atom Au-Pd nanoparticles, the prior distribution for the ECI takes the form:

$$p(\mathbf{v}) \propto \prod_{n=1}^{201} e^{\frac{-\left(V_{0,n}-V_{0,n-1}\right)^2}{2\sigma_0^2}} \tag{2}$$

where $\mathbf{v}$ is a vector containing all ECI to be fit, $p(\mathbf{v})$ is the prior probability distribution, and σ_0 is a constant to be determined via cross validation. Conceptually, this approach is analogous to connecting all pairs of values $V_{0,n}$ and $V_{0,n+1}$ with springs, where the spring constant is σ_0^{-2}.

The full prior distribution used in the Bayesian cluster expansions for this communication is the product of three terms:

$$p(\mathbf{v}) \propto \left(\prod_{\alpha \neq 0} e^{\frac{-V_\alpha^{\,2}}{2\sigma_\alpha^{\,2}}} \right) \left(\prod_{\alpha, \beta \neq \alpha} e^{\frac{-\left(V_\alpha - V_\beta\right)^2}{2\sigma_{\alpha\beta}^{\,2}}} \right) \left(\prod_{n=1}^{201} e^{\frac{-\left(V_{0,n} - V_{0,n-1}\right)^2}{2\sigma_0^{\,2}}} \right) \tag{3}$$

where the last term is given by equation (2) in the text and the first two terms are described in reference 12. For clarity an irrelevant normalization constant has been left out of the right side of equation (3). The subscripts α and β represent orbits of symmetrically equivalent clusters. Equation (3) results in the following regularization matrix, as defined in reference 12:

$$\mathbf{\Lambda} = \begin{bmatrix} \mathbf{A} & \mathbf{B} \\ \mathbf{C} & \mathbf{D} \end{bmatrix} \tag{4}$$

where $\mathbf{A}$, $\mathbf{B}$, $\mathbf{C}$, and $\mathbf{D}$ are all submatrices. $\mathbf{A}$ is a 202 × 202 matrix that represents the concentration-dependent empty ECI, with elements given by $A_{0,0} = A_{202,202} = \lambda_0$, $A_{i,i} = 2\lambda_0$ for $0 < i < 202$, $A_{i,i+1} = A_{i+1,i} = -\lambda_0$, where λ_0 is a parameter to be optimized. $\mathbf{B}$ and $\mathbf{C}$ are matrices in which all elements are 0, and $\mathbf{D}$ is the regularization matrix described in reference 12, with the row and column for the empty ECI removed.

For the Bayesian cluster expansions in this communication, the parameters λ_α and $\lambda_{\alpha\beta}$ in the regularization matrix (as defined in reference 12) are given by:

$$\begin{aligned} \lambda_\alpha &= \begin{cases} \lambda_1 \text{ for } n_\alpha = 1 \\ \lambda_2 e^{\lambda_3 r_\alpha} e^{\lambda_4 n_\alpha} \text{ for } n_\alpha > 1 \end{cases} \\ \lambda_{\alpha\beta} &= \begin{cases} \lambda_5 \lambda_\alpha \text{ if } \alpha \text{ and } \beta \text{ are congruent} \\ 0 \text{ if } \alpha \text{ and } \beta \text{ are not congruent} \end{cases} \end{aligned} \tag{5}$$

where n_α and r_α are, respectively, the number of sites per cluster in α and the maximum distance between sites in Angstroms. The regularization parameters λ_0, λ_1, λ_2, λ_3, λ_4 and λ_5 were optimized by using a conjugate gradient algorithm to minimize the leave-one-out cross-validation error. The resulting prior probability distribution encourages to the ECI to take on values that are physically more likely, but it does not impose any hard constraints. For example, $V_{0,n}$ could vary rapidly with n if the training data sufficiently support such a change. As a result, there is a dramatic reduction in the size of the training set required to reach a given level of accuracy.

For comparison with the Bayesian approaches cluster expansions were also trained using the more common cluster selection method, in which there is no regularization matrix. The set of included clusters was selected by using simulated annealing to minimize the leave-five-out cross-validation error, as this was found to result in lower prediction errors than the leave-one-out cross validation error. For every cluster included in the expansion, all subclusters were included as well.

To evaluate the Bayesian cluster expansion, density functional theory (DFT) calculations were used to generate a data set for 171 cuboctahedral 201-atom (~2 nm) Au-Pd nanoparticles. All DFT calculations were performed using the Vienna Ab-Initio Simulation Package (VASP)[18] with the Perdew-Burke-Eznerhof (PBE)[19] exchange-correlation functional. The standard projector-augmented wave (PAW)[20] potentials provided with VASP were used, and VASP was run with the precision level set to "accurate", ensuring that there were no wrap-around errors in the Fourier transforms. A

single *k*-point at the center of the Brillouin zone was used for each nanoparticle, and Gaussian smearing with a width of 0.05 eV was used to set partial occupancies. Real-space projectors were used to evaluate the non-local part of the PAW potential. Calculations were stopped when the difference for the total energy for the nanoparticle in successive ionic relaxation steps was less than 1 meV. Calculations were run in a periodic cubic cell with length of 3 nm on each side, ensuring at least 1nm between each nanoparticle and its periodic images. The surface *d*-band centers were calculated by restarting the calculations from the relaxed structures and using the projected density of states for the first two surface layers.

The set of 171 nanoparticles consisted of a set of 42 structures selected to sample configuration space in a way that minimizes the variance in the predicted property values, as described in reference 21. The remaining 129 structures were low-energy structures at different compositions predicted by the cluster expansion. Due to the importance of the end compositions on the quality of the cluster expansion,[21] the pure Au and pure Pd nanoparticles were included twice in the training set in a way that ensured that during cross-validation the cluster expansion was always fit to a set of structures that included both pure Au and pure Pd.

To demonstrate the predictive power of the Bayesian approach I have generated 10 randomly-ordered lists of the set of 171 structures. Cluster expansions were trained using the first 10 structures in each list, and the prediction error of the cluster expansion was evaluated against a test set consisting of the remaining 161 structures. The average of

these 10 prediction errors was taken to be the estimated prediction error. This process was then repeated by incrementally moving structures from the test set to the training set. The required size of the training set to reach different levels of accuracy is given in Table I. To achieve an accuracy of 5 meV/atom, the Bayesian approach with concentration-dependent ECI is about five times as efficient as cluster selection, and about twice as efficient as a Bayesian approach with concentration-independent ECI.

	5 meV / atom	4 meV / atom	3 meV /atom	2 meV / atom
Cluster Selection	118	>160	>160	>160
Bayesian with concentration-indepenent ECI	40	65	>160	>160
Bayesian with concentration-dependent ECI	24	31	46	76

Table I. The number of structures in the training set required to reach different levels of estimated prediction error.

For the comparisons listed in Table I, the set of candidate clusters included all pairs up to the second-nearest neighbor and all 3-, and 4-, site clusters up to the nearest neighbor, for a total of 102 symmetrically distinct clusters. The cluster expansion generated with the full set of 171 training structures used all pairs up to the ninth-nearest neighbor, and all 3- and 4- site clusters up to the second nearest neighbor, for a total of 398 symmetrically distinct clusters. It was found that this set of clusters slightly improved the accuracy of the Bayesian approach, resulting in a cross-validation error of 1.02 meV / atom. However it was not used for comparison with cluster selection because it made the cluster selection approach significantly worse.

There were not enough structures in the training set to evaluate higher levels of accuracy for cluster selection, but an additional data point comes from the recent work of Yuge,[22] in which a genetic algorithm[23] was used to select clusters for a cluster expansion of a 55-atom Pt-Rh nanoparticle. With 327 nanoparticles in the training set, a cross-validation error of 2.9 eV/atom was achieved. The approach outlined in this communication achieves the same average cross-validation error for a 201-atom Au-Pd nanoparticle with only 20 nanoparticles in the training set. Yuge did not report prediction error measured against an independent test set, but the estimated prediction error for the Au-Pd calculations is less than 2.9 eV/atom with only 47 structures in the training set.

The cluster expansion generated by the full set of 171 structures allows for a very accurate theoretical study of atomic order in nanoparticles. The estimated prediction error relative to DFT is approximately 1 meV per atom, which would be low for a bulk cluster expansion and is exceptionally low for a 2nm nanoparticle. I have used this cluster expansion in Monte Carlo simulations to predict both the ground state and the equilibrium room-temperature atomic order in the nanoparticles (Figure 1). The results are qualitatively similar to results obtained both experimentally and with the embedded atom potential,[24, 25] in that there is competition between the preference of Au atoms to occupy sites with low coordination and the preference for Pd atoms occupy sites adjacent to Au atoms.

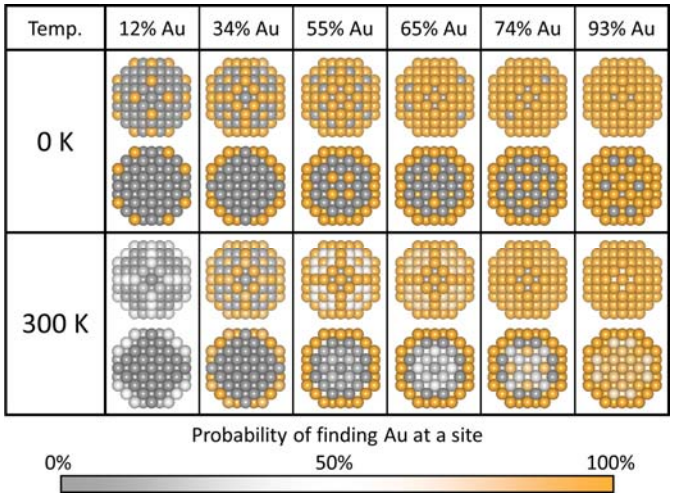

Figure 1 (Color online). Atomic ordering in Au-Pd nanoparticles. The first and third rows show the exterior of the nanoparticles, and the second and fourth rows show a cross-section of the middle of the nanoparticles.

I have extended my analysis to the electronic structure of nanoparticles. It has been shown that the binding energy of adsorbates and catalytic activity of metallic surfaces is related to the position of the center of the electronic *d* band at the surface.[26] I have calculated the surface *d*-band centers for each of the particles in the training set and trained a separate cluster expansion to predict the surface *d*-band center as a function of atomic order. The set of 398 clusters was used for the *d*-band center cluster expansion, resulting in a cross-validation error of 7 meV. The two cluster expansions (of energies and *d*-band centers) were used in a Monte Carlo simulation to predict the equilibrium distribution of *d*-band centers in an ensemble of nanoparticles at 300K. The results are shown in Figure 2. These results can only be obtained by using a method that is able to simultaneously rapidly evaluate the atomic and electronic structure of the nanoparticles.

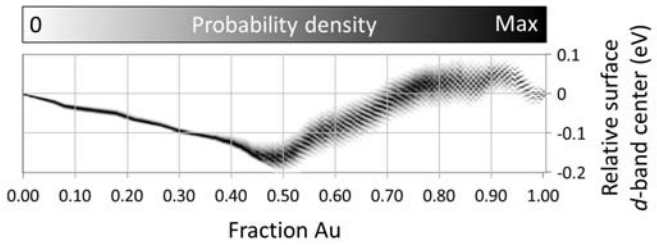

Figure 2. Surface *d*-band centers as a function of composition at 300K**.** The *y*-axis shows the deviation of the surface *d*-band center from a linear interpolation of the surface *d*-band centers of pure Au and pure Pd particles. At each composition, the predicted thermodynamic spread in surface *d*-band centers for an ensemble of nanoparticles is shown.

Atomic-level details of the surface structure are also important predictors of catalytic activity. For example, it is known that the rate of the acetoxylation of ethylene on Au-Pd surfaces depends on the spacing between Pd monomers on the surface.[27] Similarly, hydrogen adsorption on the $\{111\}$ surface of Au-Pd nanoparticles requires the existence of Pd dimers on the surface.[28] The cluster expansion enables accurate prediction of the atomic arrangement on the nanoparticle surface as a function of composition and temperature. The fractions of Au-Au dimers, Au-Pd dimers, and Pd-Pd dimers on the $\{111\}$ surfaces at 300K are shown in Figure 3. The ability to rapidly and accurately predict equilibrium electronic and atomic structure as a function of composition and temperature should make this approach very useful for the design of new catalysts.

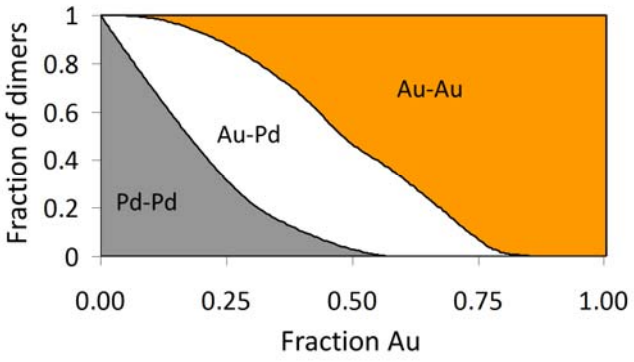

Figure 3 (Color online). Dimer distribution on the $\{111\}$ surface at 300K**.** The x-axis is the total fraction of Au in the nanoparticle, and the y-axis is the fraction of nearest-neighbor dimers.

In this communication I have demonstrated that for DFT calculations on alloy nanoparticles, the Bayesian approach to creating cluster expansions reduces the computational cost to reach a given level of accuracy by nearly an order of magnitude relative to cluster selection. To account for significant composition-dependent effects, the previously-presented Bayesian cluster expansion method has been extended to allow for composition-dependent ECI. As a result, it is possible to accurately predict structure-property relationships in multi-nanometer alloy nanoparticles with reasonable computational cost. This approach should be a valuable tool for researchers seeking to accelerate the development of new technologies through the rational design of nanoscale materials.

Acknowledgements

This work was performed in part on TeraGrid supercomputers using supercomputing grants from the U.S. National Science Foundation. This project was funded by the U.S. Department of Energy under grant DE-FG02-96ER45571.

References

[1] N. Meethong, H. Y. S. Huang, W. C. Carter, and Y. M. Chiang, Electrochemical and Solid State Letters **10**, A134 (2007).

[2] S. H. Sun, C. B. Murray, D. Weller, L. Folks, and A. Moser, Science **287**, 1989 (2000).

[3] S. Alayoglu, A. U. Nilekar, M. Mavrikakis, and B. Eichhorn, Nature Materials **7**, 333 (2008).

[4] V. R. Stamenkovic, B. Fowler, B. S. Mun, G. F. Wang, P. N. Ross, C. A. Lucas, and N. M. Markovic, Science **315**, 493 (2007).

[5] S. J. L. Billinge and I. Levin, Science **316**, 561 (2007).

[6] W. Kohn and L. J. Sham, Phys. Rev. **140**, A1133 (1965).

[7] J. M. Sanchez, F. Ducastelle, and D. Gratias, Physica **128A**, 334 (1984).

[8] E. Ising, Zeitschrift für Physik **31**, 253 (1925).

[9] A. van de Walle and G. Ceder, J. of Phase Equilibria **23**, 348 (2002).

[10] S. Q. Wei and M. Y. Chou, Physical Review B **50**, 4859 (1994).

[11] T. Mueller and G. Ceder, ACS Nano **4**, 5647 (2010).

[12] T. Mueller and G. Ceder, Physical Review B **80**, 024103 (2009).

[13] M. S. Daw and M. I. Baskes, Physical Review B **29**, 6443 (1984).

[14] A. Gonis, P. P. SIngh, P. E. A. Turchi, and X. G. Zhang, Phys. Rev. B **51**, 2122 (1995).

[15] J. M. Sanchez, Physical Review B **81**, 224202 (2010).

[16] M. Asta, C. Wolverton, D. Defontaine, and H. Dreysse, Physical Review B **44**, 4907 (1991).

[17] C. Wolverton, M. Asta, H. Dreysse, and D. Defontaine, Physical Review B **44**, 4914 (1991).

[18] G. Kresse and J. Furthmuller, Phys. Rev. B **54**, 11169 (1996).

[19] J. P. Perdew, K. Burke, and M. Ernzerhof, Physical Review Letters **77**, 3865 (1996).

[20] P. E. Blochl, Physical Review B **50**, 17953 (1994).

[21] T. Mueller and G. Ceder, Physical Review B **82**, 184107 (2010).

[22] K. Yuge, Physical Review B **84**, 085451 (2011).

[23] G. L. W. Hart, V. Blum, M. J. Walorski, and A. Zunger, Nature Materials **4**, 391 (2005).

[24] S. J. Mejia-Rosales, C. Fernandez-Navarro, E. Perez-Tijerina, D. A. Blom, L. F. Allard, and M. Jose-Yacaman, J. Phys. Chem. C **111**, 1256 (2007).

[25] I. Atanasov and M. Hou, Surface Science **603**, 2639 (2009).

[26] H. B and N. J. K, Surf. Sci. **343**, 211 (1995).

[27] M. S. Chen, D. Kumar, C. W. Yi, and D. W. Goodman, Science **310**, 291 (2005).

[28] F. Maroun, F. Ozanam, O. M. Magnussen, and R. J. Behm, Science **293**, 1811 (2001).